

COUPLED MODE MODELING IN GUIDED-WAVE PHOTONICS: A VARIATIONAL, HYBRID ANALYTICAL-NUMERICAL APPROACH

Manfred Hammer

University of Twente, MESA⁺-Institute for Nanotechnology, P.O. Box 217, 7500 AE Enschede, The Netherlands
m.hammer@math.utwente.nl

Abstract – A general variant of coupled-mode-theory for frequency domain guided wave problems in integrated optics is discussed. Starting point is a physically reasonable field template, that typically consists of a few known, most relevant modes of the optical channels in the structure, superimposed with coefficient functions of the respective — in principle arbitrary — propagation coordinates. Discretization of these unknown functions into 1-D finite elements leads to an approximation of the optical field in terms of a linear superposition of structure-adapted, more or less localized modal elements. By variational restriction of a functional representation of the full 2-D/3-D vectorial first order frequency domain Maxwell equations (with transparent influx boundary conditions for inhomogeneous exterior), one can then reduce the problem to a small- to moderate-sized system of linear equations. 2-D examples for a crossing of dielectric waveguides and a grating-assisted rectangular resonator illustrate the performance of the approach.

I. INTRODUCTION

A certain class of photonic devices are distinguished by the following common feature: The optical electromagnetic field can be described adequately by the propagation and interaction of a few known or conveniently computable basic fields, typically guided modes supported by the local optical channels. It is usually straightforward to write a reasonable ansatz for the optical field by superimposing the respective basis fields with coefficient functions that vary along the associated propagation coordinate. One obtains — necessarily approximate — equations for the varying amplitudes and their solutions. Approaches of this kind are usually called “coupled mode theory” (CMT); overviews of the rich variety of variants can be found in [1, 2], or in the textbooks [3, 4, 5, 6].

The CMT equations typically permit analytical solutions only in special situations, e.g. for longitudinally homogeneous systems of few waveguides. For other configurations one obtains higher dimensional systems of coupled differential equations, or systems with non-constant coefficients, that require numerical means. In those, by no means less interesting, cases the solutions are numerical approximations of the CMT coefficient functions, that still allow to examine the amplitude evolutions. “CMT” as it is used here encompasses explicitly these situations.

Ref. [1] classifies the existing methods for linear structures as codirectional CMT (codirectional propagation of modes along more or less parallel waveguide cores) and contradirectional CMT (corrugated channels, waveguide gratings). Light propagation is modeled from a viewpoint of mode amplitude evolution along a single propagation coordinate, i.e. through sets of coupled ordinary differential equations. One also frequently comes across purely phenomenological models, where coupling coefficients are treated as fit-parameters.

This paper briefly reviews a CMT variant that to some degree generalizes the former properties, by variational means in combination with simple numerics. The method starts from first principles, i.e. with the frequency domain Maxwell equations for a given optical structure. Beyond the CMT template no further heuristics is required to arrive at the desired approximations for the optical field. Further details on this Hybrid analytical/numerical Coupled Mode Theory (HCMT) are given in Ref. [7].

II. HYBRID ANALYTICAL / NUMERICAL COUPLED MODE THEORY

The HCMT approach will be explained along the 2-D example of Figure 1. Nevertheless, we adopt a notation that applies directly also to three spatial dimensions. The frequency domain equations

$$\nabla \times \mathbf{H} - i\omega\epsilon_0\epsilon\mathbf{E} = 0, \quad -\nabla \times \mathbf{E} - i\omega\mu_0\mathbf{H} = 0. \quad (1)$$

are considered for a structure with relative dielectric permittivity ϵ , for vacuum permittivity ϵ_0 and permeability μ_0 , where the optical electric and magnetic fields \mathbf{E} , \mathbf{H} vary harmonically in time $\sim \exp(i\omega t)$ with angular frequency $\omega = 2\pi c/\lambda$, always specified by the vacuum wavelength λ , for vacuum speed of light c .

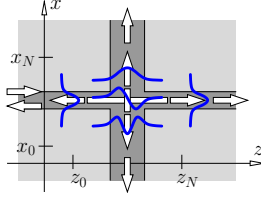


Fig. 1: A perpendicular crossing of two waveguide cores. The 2-D problem is described in Cartesian coordinates x, z . The computational window $x \in [x_0, x_N]$, $z \in [z_0, z_N]$ covers the region of interest around the waveguide intersection. Directional variants of the guided modes supported by the two channels serve as basis fields for the HCMT model.

A. Template for the Coupled Mode Field

Starting point for the CMT analysis is a physically plausible and, as far as possible, also convenient template for the optical electromagnetic field. For the example of Figure 1 one expects the following interaction to take place around the center of the crossing: An incoming guided mode, entering the horizontal channel from the left, is partly reflected and / or transmitted into other guided modes of the horizontal core, and it transfers part of its power to modes supported by the vertical waveguide that travel upward or downward. Hence, if we disregard the radiative power loss to nonguided waves, a reasonable CMT field template could read:

$$\begin{pmatrix} \mathbf{E} \\ \mathbf{H} \end{pmatrix}(x, z) = \sum_m f_m(z) \psi_m^f(x, z) + \sum_m b_m(z) \psi_m^b(x, z) + \sum_m u_m(x) \psi_m^u(x, z) + \sum_m d_m(x) \psi_m^d(x, z). \quad (2)$$

Here the symbols ψ_m^{\cdot} with upper indices f,b denote the forward or backward propagating variant of the mode of order m of the horizontal core with electric part $\tilde{\mathbf{E}}_m^{\text{f,b}}$ and magnetic part $\tilde{\mathbf{H}}_m^{\text{f,b}}$ of the mode profile. These are functions of the transverse coordinate x , with exponential z -dependences with propagation constant $\mp\beta_m^{\text{h}}$:

$$\psi_m^{\text{f,b}}(x, z) = \begin{pmatrix} \tilde{\mathbf{E}} \\ \tilde{\mathbf{H}} \end{pmatrix}_m^{\text{f,b}}(x) e^{\mp i\beta_m^{\text{h}}z}, \quad \psi_m^{\text{u,d}}(x, z) = \begin{pmatrix} \tilde{\mathbf{E}} \\ \tilde{\mathbf{H}} \end{pmatrix}_m^{\text{u,d}}(z) e^{\mp i\beta_m^{\text{v}}x}. \quad (3)$$

Analogously, indices u, d identify the upward or downward traveling modes of the vertical waveguide, with propagation constants $\mp\beta_m^{\text{v}}$. It remains to determine the modal amplitudes f_m, b_m, u_m, d_m , which are functions of the respective horizontal coordinate z (f_m, b_m) or of the vertical coordinate x (u_m, d_m).

We like to emphasize that the procedure outlined below applies just as well to a variety of other structures, provided that it is possible to write down a field template in the form of Eq. (2), i.e. a superposition of given fields with amplitudes that are each a function of some propagation coordinate. These need not necessarily be Cartesian coordinates: the waves inside a circular microcavity, for instance, would most conveniently be described by bend modes, i.e. in terms of polar coordinates [8, 9, 10]. For certain problems, e.g. if one includes resonances (quasi-normal modes, QNMs) of a high-Q microcavity as basis elements ψ , single coefficients without dependence on a propagation coordinate could be adequate [11]. In that case the discretization step (next section) is omitted for the respective terms in the template and one arrives directly at the abstract form (5).

B. Discretization of Amplitude Functions

Standard 1-D first order finite elements (FEs) are now used to discretize the unknown functions. As an example, the amplitude $f_m(z)$ of the m -th order forward mode of the horizontal channel is expanded as

$$f_m(z) = \sum_{j=0}^N f_{m,j} \alpha_j(z). \quad (4)$$

For $j = 1, \dots, N-1$ the α_j are standard triangle functions; α_0 and α_N , with nodes at the boundaries at z_0, z_N of the computational interval, are 1 in the respective half-infinite exteriors. Observe that $f_{m,0}$, the input amplitude of the mode of order m at the left boundary, is actually a given quantity, while all other coefficients are so far unknown. Analogous discretization procedures apply to b_m, u_m , and d_m , in the last two cases with respect to x .

This done, the ansatz for the full electromagnetic field assumes the abstract form

$$\begin{pmatrix} \mathbf{E} \\ \mathbf{H} \end{pmatrix}(x, z) = \sum_k a_k(\alpha(\cdot) \psi(\cdot)(x, z)) =: \sum_k a_k \begin{pmatrix} \mathbf{E}_k \\ \mathbf{H}_k \end{pmatrix}(x, z), \quad (5)$$

Here the formal index k distinguishes waveguide channels, propagation directions, mode orders, and element numbers, indicated by the wildcards (dots) in the second term. Element functions α and mode fields ψ are combined into modal elements, the quantities $(\mathbf{E}_k, \mathbf{H}_k)$ in the last term. The unknowns and given values of the previous separate expansions reappear as expansion coefficients $a_k \in \{f_{m,j}, b_{m,j}, u_{m,j}, d_{m,j}\}$

C. Variational Form of the Scattering Problem

Consider the abstract 3-D guided-wave scattering problem as introduced schematically in Figure 2. The frequency domain equations (1) are to be solved inside the computational domain Ω .

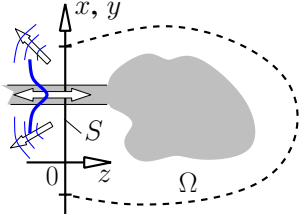


Fig. 2: An exemplary port plane S constitutes part of the boundary of the domain Ω . Axes x and y of a local coordinate system span S , the z -axis is oriented towards the interior of Ω . Incoming waveguides are parallel to the z -axis, i.e. the exterior is z -homogeneous. Extension to further input/output ports should be straightforward.

Transparent influx boundary conditions (TIBCs) for the electromagnetic fields \mathbf{E} , \mathbf{H} (transverse components only) on S can be stated formally as [7]

$$\mathbf{E} = \sum_m 2F_m \tilde{\mathbf{E}}_m - \sum_m \frac{1}{N_m} \langle \tilde{\mathbf{E}}_m, \mathbf{H} \rangle \tilde{\mathbf{E}}_m, \quad \mathbf{H} = \sum_m 2F_m \tilde{\mathbf{H}}_m - \sum_m \frac{1}{N_m} \langle \mathbf{E}, \tilde{\mathbf{H}}_m \rangle \tilde{\mathbf{H}}_m. \quad (6)$$

Here $(\tilde{\mathbf{E}}_m, \tilde{\mathbf{H}}_m)$ are the electric and magnetic profiles of the complete set of normal modes [4] on S (partly continuous and partly discrete index m , the combination $(\tilde{\mathbf{E}}_m, \tilde{\mathbf{H}}_m)$ represents a wave that travels towards the interior of Ω). Orthogonality properties $\langle \tilde{\mathbf{E}}_l, \tilde{\mathbf{H}}_k \rangle = \delta_{lk} N_k$ hold, with nonzero N_k , for the product $\langle \mathbf{A}, \mathbf{B} \rangle = \iint_S (\mathbf{A} \times \mathbf{B}) \cdot \mathbf{e}_z \, dx \, dy$. Coefficients F_m specify the external influx, already projected onto the local modal basis.

A variational representation of the former problem is given by the functional [7]

$$\begin{aligned} \mathcal{F}(\mathbf{E}, \mathbf{H}) &= \iiint_{\Omega} \{ \mathbf{E} \cdot (\nabla \times \mathbf{H}) + \mathbf{H} \cdot (\nabla \times \mathbf{E}) - i\omega\epsilon_0 \mathbf{E}^2 + i\omega\mu_0 \mathbf{H}^2 \} \, dx \, dy \, dz \\ &- \sum_m 2F_m \left\{ \langle \tilde{\mathbf{E}}_m, \mathbf{H} \rangle - \langle \mathbf{E}, \tilde{\mathbf{H}}_m \rangle \right\} + \sum_m \frac{1}{2N_m} \left\{ \langle \tilde{\mathbf{E}}_m, \mathbf{H} \rangle^2 - \langle \mathbf{E}, \tilde{\mathbf{H}}_m \rangle^2 \right\} \end{aligned} \quad (7)$$

(an expression from [4], extended by the boundary integrals; cf. the formulation for scalar 1-D and 2-D second order systems with homogeneous exterior of [12, 13]). If \mathcal{F} becomes stationary, then \mathbf{E} and \mathbf{H} satisfy Eqs. (1) in Ω , they satisfy the TIBCs (6) on S , and the transverse components of both \mathbf{E} and \mathbf{H} vanish on all other parts $\partial\Omega \setminus S$ of the boundary.

D. Solution by Variational Restriction

Upon insertion of expression (5), the functional \mathcal{F} becomes a function of the coefficients $\mathbf{a} = (\dots, a_k, \dots)$ of the modal elements. The restricted function $\mathcal{F}_r(\mathbf{a})$ is quadratic in these unknowns, with an additional linear term,

$$\mathcal{F}_r(\mathbf{a}) = \sum_{l,k} a_l a_k F_{lk} + \sum_l a_l R_l + \sum_{l,k} a_l a_k B_{lk} = \mathbf{a} \cdot \mathbf{F} \mathbf{a} + \mathbf{R} \cdot \mathbf{a} + \mathbf{a} \cdot \mathbf{B} \mathbf{a}, \quad (8)$$

where the matrices / the vector \mathbf{F} , \mathbf{R} and \mathbf{B} are formed by integrals of products of modal elements over the interior (\mathbf{F}) or the port plane (\mathbf{R} , \mathbf{B}); prescribed amplitudes of the input waves are included in \mathbf{R} . Note that frequently, depending on the problem at hand, only a few terms in the formal sums of Eq. (6) are relevant, due to modal orthogonality properties.

To identify an optimum approximation, given the degrees of freedom in the field template (5), one now requires the restricted functional (8) to become stationary. The first variation of \mathcal{F}_r vanishes

$$\delta \mathcal{F}_r = \delta \mathbf{a} \cdot \left((\mathbf{M} + \mathbf{M}^T) \mathbf{a} + \mathbf{R} \right) = 0, \quad \mathbf{M} = \mathbf{F} + \mathbf{B}, \quad (9)$$

for arbitrary variations $\delta \mathbf{a}$, if the optimum vector of coefficients solves the linear system

$$\left(\mathbf{M} + \mathbf{M}^T \right) \mathbf{a} + \mathbf{R} = 0. \quad (10)$$

Modal output amplitudes are already included in these unknowns; evaluation of Eqs. (2), (4) permits to assemble the full HCMT field approximation. The algebraic procedure can be refined by observing that some components of \mathbf{a} are actually given quantities; Eq. (10) then represents an overdetermined system. The least squares solution [7] turns out to be beneficial for the smoothness of the results.

As an alternative one can apply a Galerkin procedure to assign values to the coefficients in the general FE-CMT expansion (5). For convenience the formalism then employs a weak form of Eqs. (1) with field products where one factor appears as a complex conjugate, which has certain practical advantages [4]. That form, however, appears not to be related to a variational principle. Further comments on both approaches are given in Ref. [7].

III. NUMERICAL RESULTS

Figures 3, 4 summarize HCMT results for the 2-D waveguide crossing, and for a grating assisted resonator from Ref. [14]. In both cases, reference data has been generated by rigorous, quasi-analytical bidirectional or quadridi-rectional eigenmode propagation methods (BEP, [15, 16]; QUEP [17]; [18]). The crossing example clearly shows that a coupled mode approach can be implemented successfully without the concept of field evolution along a common propagation coordinate. Still, in terms of their FE discretization, the amplitude functions (Figure 3(a)) are available for inspection and a discussion of the mode interaction.

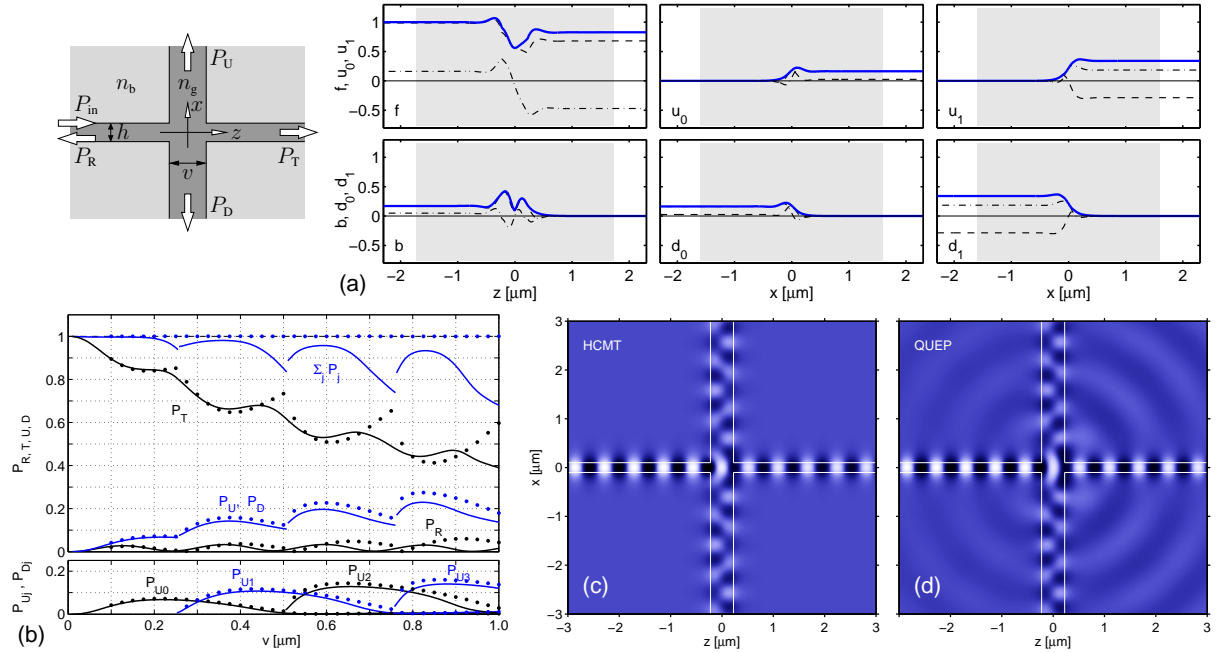


Fig. 3: Perpendicular waveguide intersection: A vertical core of variable width v with refractive indices $n_g = 3.4$ (cores) and $n_b = 1.45$ (background) crosses a horizontal waveguide with thickness $h = 0.2 \mu\text{m}$. The propagation of TE polarized light at a vacuum wavelength $\lambda = 1.55 \mu\text{m}$ is considered. (a), HCMT simulation, $v = 0.45 \mu\text{m}$: Amplitude functions f , b of the right- and left-traveling fundamental modes in the horizontal channel (first column), and functions u_m , d_m of the upward and downward propagating modes of order $m = 0, 1$ of the vertical channel (second and third columns). Field plots, for $v = 0.45 \mu\text{m}$: physical time snapshots of the principal component E_y of the TE fields as predicted by the present procedure (HCMT, (b)) and by rigorous mode expansion simulations (QUEP, (d), reference [17]). (e): Guided power transmission versus the width v of the vertical core, HCMT results (dots) and QUEP simulations (lines, reference [17]). For unit input in the left channel, P_R , P_T , P_U , and P_D are the relative power fractions carried by guided modes that leave the crossing along the left, right, upper, and lower channel. The top plot shows also the sum of these quantities. Lower inset: power fractions $P_{U_m} = P_{D_m}$ associated with guided modes of order $m = 0, 1, 2, 3$ of the multimode vertical channel.

The standing wave resonator of Figure 4 is intended as (part of [19, 14]) an integrated optical add-drop-wavelength filter. We have recently investigated a 2-D variant of this concept [14], meant as an alternative to conventional circular, ring- or disk-shaped microresonators. The device shows the advantages of mainly bidirectional light propagation (opening possibilities for electrooptic tuning by materials with pronounced anisotropy), of a long interaction length between the cavity and the bus waveguides (fabrication tolerance of the coupler gap), and of additional design freedom concerning the reflector gratings (realization of a device that supports only a single resonance [14]), at the price of a relatively large length, and of the necessity of the grating fabrication.

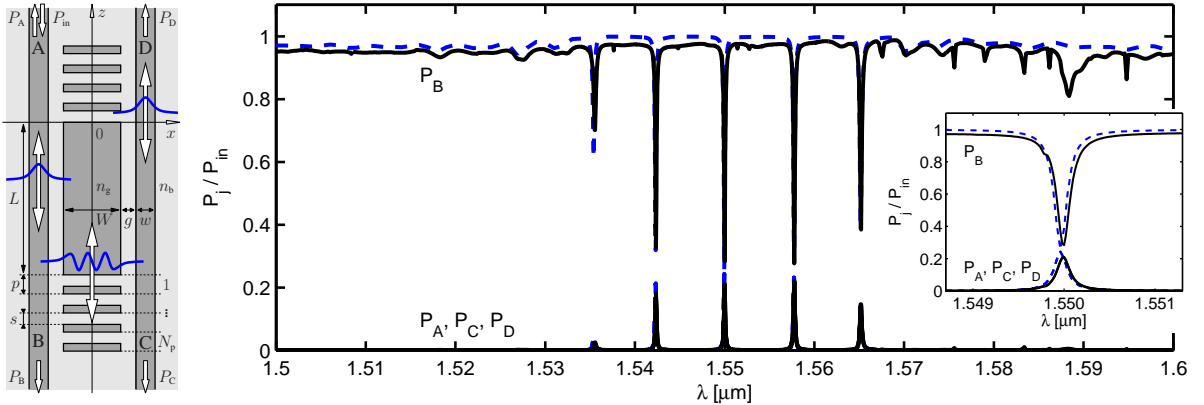


Fig. 4: Spectral response of a grating assisted rectangular resonator: Two parallel waveguide cores of width w are coupled by a cavity of width W and length L , separated by gaps g . Gratings with N_p periods of length p with a spacing s enclose the cavity. The guiding regions with refractive index n_g are embedded in a background medium with index n_b . The set of example parameters from Ref. [14] leads to a pronounced resonance at the vacuum wavelength $\lambda = 1.55 \mu\text{m}$: $n_g = 1.6$, $n_b = 1.45$, $w = 1.0 \mu\text{m}$, $g = 1.6 \mu\text{m}$, $W = 9.955 \mu\text{m}$, $L = 79.985 \mu\text{m}$, $p = 1.538 \mu\text{m}$, $s = 0.281 \mu\text{m}$, $N_p = 40$. P_A to P_D are the relative power fractions that are reflected or transmitted into ports A to D. Note that the curves related to P_A , P_C , and P_D are almost completely superimposed. Bold lines (reference) correspond to rigorous mode expansion computations [15, 16], the dashed lines indicate the HCMT results. The resonator is excited in port A by the guided mode of the left core. For most wavelengths, most of the input power is directly transmitted to port B. Resonant states appear as a drop in P_B and a simultaneous increase of the reflected and dropped power fractions P_A , P_C , and P_D .

Figure 4 compares rigorous and HCMT results [7] for the spectral response of the filter device. The HCMT model combines bidirectional variants of the single guided modes of the separate bus waveguides with the forward and backward propagating 5th-order mode of the wide central core. In contrast to standard 2-D CMT models [20, 14], where one has to patch up different (co- and contradirectional) variants of CMT formulations, the present approach covers directly the codirectional coupling for the bidirectional propagation along the inner cavity segment ($z \in [0, L]$) as well as the co- and contradirectional interaction of waves of all three cores along the reflector gratings.

Note that these examples and also others in Ref. [7] cover structures with moderate to high refractive index contrast. The range of applicability of CMT-like approaches need not be restricted to “low contrast” structures. Rather these techniques, including the one discussed here, are applicable where one can reasonably expect relatively weak or only localized mutual perturbations of the interacting basis modes, such that the optical fields can well be described by the CMT field templates.

IV. CONCLUDING REMARKS

In contrast to most established variants, coupled mode *equations* do not appear in the version of coupled mode theory as outlined above. Rather than deriving systems of coupled ordinary differential equations and solving these numerically (or analytically, at the price of serious additional approximations), the present variational approach permits to step directly from the CMT field template towards a system of algebraic equations for the numerical FE approximation of the coupled mode amplitude functions. This allows for a quite general, straightforward, and uniform formulation that promises to be applicable to some range of problems in two and prospectively also three spatial dimensions.

The form of the template (5) covers in principle also rigorous numerical discretizations of the optical fields. Hence this may be viewed as a numerical finite element technique with highly specialized, structure-adapted elements (the former modal elements). The method can only converge towards a continuous amplitude approximation (2), rather than towards the true physical solution. In return one employs 1-D FE discretizations with only quite few unknowns, when compared to standard 2-D or 3-D FE settings. As much as possible of the physics is already built into the elements, leading to small or moderate sized algebraic systems.

ACKNOWLEDGMENT

This work has been supported by the Dutch Technology foundation (BSIK / NanoNed project TOE.7143).

REFERENCES

- [1] D. G. Hall and B. J. Thompson, editors. *Selected Papers on Coupled-Mode Theory in Guided-Wave Optics*, volume MS 84 of *SPIE Milestone Series*. SPIE Optical Engineering Press, Bellingham, Washington USA, 1993.
- [2] W. P. Huang. Coupled mode theory for optical waveguides: an overview. *Journal of the Optical Society of America A*, 11(3):963–983, 1994.
- [3] A. W. Snyder and J. D. Love. *Optical Waveguide Theory*. Chapman and Hall, London, New York, 1983.
- [4] C. Vassallo. *Optical Waveguide Concepts*. Elsevier, Amsterdam, 1991.
- [5] R. März. *Integrated Optics — Design and Modeling*. Artech House, Boston, London, 1994.
- [6] K. Okamoto. *Fundamentals of Optical Waveguides*. Academic Press, San Diego, 2000.
- [7] M. Hammer. Hybrid analytical / numerical coupled-mode modeling of guided wave devices. *Journal of Lightwave Technology*, 25(9):2287–2298, 2007.
- [8] K. R. Hiremath, M. Hammer, R. Stoffer, L. Prkna, and J. Čtyroký. Analytical approach to dielectric optical bent slab waveguides. *Optical and Quantum Electronics*, 37(1-3):37–61, 2005.
- [9] K. R. Hiremath, R. Stoffer, and M. Hammer. Modeling of circular integrated optical microresonators by 2-D frequency-domain coupled mode theory. *Optics Communications*, 257(2):277–297, 2006.
- [10] R. Stoffer, K. R. Hiremath, M. Hammer, L. Prkna, and J. Čtyroký. Cylindrical integrated optical microresonators: Modeling by 3-D vectorial frequency domain coupled mode theory. *Optics Communications*, 256(1–3):46–67, 2005.
- [11] M. Maksimovic, M. Hammer, and E. van Groesen. Field representation for optical defect microcavities in multilayer structures using quasi-normal modes. *Optics Communications*, 281(6):1401–1411, 2008.
- [12] A. Sopaheluwakan. *Characterization and Simulation of Localized States in Optical Structures*. University of Twente, Enschede, The Netherlands, 2006. Ph.D. Thesis.
- [13] E. W. C. van Groesen and J. Molenaar. *Continuum Modeling in the Physical Sciences*. SIAM publishers, Philadelphia, USA, 2007.
- [14] M. Hammer, D. Yudistira, and R. Stoffer. Modeling of grating assisted standing wave microresonators for filter applications in integrated optics. *Optical and Quantum Electronics*, 36(1–3):25–42, 2004.
- [15] M. Lohmeyer and R. Stoffer. Integrated optical cross strip polarizer concept. *Optical and Quantum Electronics*, 33(4/5):413–431, 2001.
- [16] M. Lohmeyer. Mode expansion modeling of rectangular integrated optical microresonators. *Optical and Quantum Electronics*, 34(5):541–557, 2002.
- [17] M. Hammer. Quadridirectional eigenmode expansion scheme for 2-D modeling of wave propagation in integrated optics. *Optics Communications*, 235(4–6):285–303, 2004.
- [18] M. Hammer. METRIC — Mode expansion tools for 2D rectangular integrated optical circuits. <http://www.math.utwente.nl/~hammer/Metric/>.
- [19] C. Manolatu, M. J. Khan, S. Fan, P. R. Villeneuve, H. A. Haus, and J. D. Joannopoulos. Coupling of modes analysis of resonant channel add-drop filters. *IEEE Journal of Quantum Electronics*, 35(9):1322–1331, 1999.
- [20] M. Hammer. Resonant coupling of dielectric optical waveguides via rectangular microcavities: The coupled guided mode perspective. *Optics Communications*, 214(1–6):155–170, 2002.